DMD Fast Forward. Published on February 25, 2010 as doi:10.1124/dmd.109.031583

Identification of novel metabolic pathways of pioglitazone in hepatocytes: *N*-glucuronidation of thiazolidinedione ring and sequential ring opening pathway

Minoru Uchiyama, Thomas Fischer, Juergen Mueller, Minoru Oguchi, Naotoshi Yamamura, Hiroko Koda, Haruo Iwabuchi, and Takashi Izumi

Drug Metabolism & Pharmacokinetics Research Laboratories, Daiichi Sankyo Co., Ltd., Tokyo, Japan (M.U., N.Y., H.K., H.I., T.I.); Drug Metabolism Department, Daiichi Sankyo Europe GmbH., Martinsried, Germany (T.F., J.M.); and Research Department I, Daiichi Sankyo RD Associe Co., Ltd., Tokyo, Japan (M.O.)

DMD Fast Forward. Published on February 25, 2010 as DOI: 10.1124/dmd.109.031583
This article has not been copyedited and formatted. The final version may differ from this version.

Running Title: Identification of novel metabolites of pioglitazone

Address correspondence to:

Takashi Izumi

Drug Metabolism & Pharmacokinetics Research Laboratories, Daiichi Sankyo Co., Ltd., 1-2-58 Hiromachi, Shinagawa-Ku, Tokyo, 140-8710, Japan

Tel: +81-3-3492-3131

Fax: +81-3-5436-8567

E-mail: izumi.takashi.ka@daiichisankyo.co.jp

Text Pages: 29

Tables: 1

Figures: 12

References: 32

Abstract: 215 words

Introduction: 362 words

Discussion: 789 words

Abbreviations: LC/MS/MS, liquid chromatography/tandem mass spectrometry; PPARγ, peroxisome proliferator-activated receptor gamma; HBSS, Hank's balanced salt solution; EGTA, ethyleneglycol-bis-aminoethylether-*N*,*N*,*N'*,*N'*-tetraacetic acid; SAM, *S*-adenosyl-L-methionine; DMSO, dimethyl sulfoxide; HEPES, *N*-2-hydroxy

DMD Fast Forward. Published on February 25, 2010 as DOI: 10.1124/dmd.109.031583
This article has not been copyedited and formatted. The final version may differ from this version.

ethylpiperadine-*N'*-2-ethanosulfonic acid; HPLC, high-performance liquid chromatography; ^{1}H NMR, proton nuclear magnetic resonance; TLC, thin layer chromatography; UV, ultraviolet; MS, mass spectrometry; TFA, trifluoroacetic acid; HTCR, Human Tissue and Cell Research; radio-HPLC, radioactivity detection-HPLC; ESI, electrospray ionization; PDA, photodiode array; CID, collision-induced dissociation.

DMD Fast Forward. Published on February 25, 2010 as DOI: 10.1124/dmd.109.031583
This article has not been copyedited and formatted. The final version may differ from this version.

Abstract

The metabolism of [^{14}C]pioglitazone was studied in vitro in incubations with freshly isolated human, rat, and monkey hepatocytes. Radioactivity detection high-performance liquid chromatography analysis of incubation extracts showed the detection of thirteen metabolites (M1–M13) formed in incubations with human hepatocytes. An identical set of metabolites (M1–M13) was also detected in monkey hepatocytes. However, in rat hepatocytes, M1–M3, M5–M7, M9–M11, and M13 were also detected, but M4, M8, and M12 were not detected. The structures of the metabolites were elucidated by liquid chromatography/tandem mass spectrometry using electrospray ionization. Novel metabolites of pioglitazone detected using these methods included thiazolidinedione ring-opened methyl sulfoxide amide (M1), thiazolidinedione ring-opened *N*-glucuronide (M2), thiazolidinedione ring-opened methyl sulfone amide (M3), thiazolidinedione ring *N*-glucuronide (M7), thiazolidinedione ring-opened methylmercapto amide (M8), and thiazolidinedione ring-opened methylmercapto carboxylic acid (M11). In summary, based on the results from these studies, two novel metabolic pathways for pioglitazone in hepatocytes are proposed to be: 1) *N*-glucuronidation of the thiazolidinedione ring of pioglitazone to form M7 followed by hydrolysis to M2, and methylation of the mercapto group of the thiazolidinedione ring-opened mercapto carboxylic acid to form M11; and 2) methylation of the mercapto group of the thiazolidinedione ring-opened mercapto amide to form M8, oxidation of M8 to form M1, and oxidation of M1 to form M3.

DMD Fast Forward. Published on February 25, 2010 as DOI: 10.1124/dmd.109.031583
This article has not been copyedited and formatted. The final version may differ from this version.

Introduction

The thiazolidinedione-containing drug, pioglitazone (Fig. 1) is used in the treatment of type 2 diabetes mellitus (Chilcott et al., 2001). Pioglitazone is a member of the thiazolidinedione class agents, glitazones, and increases insulin sensitivity in target tissues by way of interaction with the peroxisome proliferator-activated receptor gamma (PPARγ) (Sood et al., 2000). Several metabolites of pioglitazone in animals and humans have been reported (Krieter et al., 1994; Kiyota et al., 1997; Maeshiba et al., 1997; Shen et al., 2003). Five primary metabolic pathways are involved and the most important cytochrome P-450 isoenzymes appear to be CYP2C8/9 and CYP3A4 (Eckland and Danhof, 2000; Baba, 2001; Jaakkola et al., 2006; Muschler et al., 2009).

Another thiazolidinedione-containing drug, troglitazone, was withdrawn from the market because of rare but serious cases of idiosyncratic hepatotoxicity (Gale, 2001; Graham et al., 2003). The generation of many reactive metabolites has been proposed in the in vitro metabolic experiments with troglitazone to investigate the relationship to the hepatotoxicity (Kassahun et al., 2001; Tettey et al., 2001; Yamamoto et al., 2002; Smith, 2003; He et al., 2004; Alvarez-Sanchez et al., 2006). By liquid chromatography/tandem mass spectrometry (LC/MS/MS) analysis, Kassahun et al. found that a sulfoxide, an α-ketoisocyanate, and a sulfenic acid of troglitazone were generated as reactive intermediates that easily react with glutathione in human liver microsomes or a human recombinant CYP3A4 system. Based on the discovery of the reactive metabolites and the presumed metabolic pathway, Kassahun et al. also reported the possible contribution of the reactive metabolites to the hepatotoxicity of troglitazone.

For pioglitazone, the reactive intermediates of pioglitazone and their presumed metabolic pathway, which is similar to that of troglitazone, were also reported (Baughman et al., 2005). They have identified the oxidative thiazolidinedione ring-opened products of pioglitazone (M-X) in rat and human liver microsomes. In addition, they have identified its ring-opened glutathione conjugates of pioglitazone (M-A and M-B) in rat and human liver microsomes and suspensions of freshly isolated rat hepatocytes.

In this study, we performed a detailed characterization of the metabolites of pioglitazone by employing hepatocyte incubation, radioactivity detection high-performance liquid chromatography (radio-HPLC), and LC/MS/MS techniques in order to understand further the potential metabolic pathways of the drug.

DMD Fast Forward. Published on February 25, 2010 as DOI: 10.1124/dmd.109.031583
This article has not been copyedited and formatted. The final version may differ from this version.

Materials and Methods

Materials.

Radiolabeled [thiazolidinedione-5-^{14}C]pioglitazone (specific radioactivity: 20 mCi/mmol, radiochemical purity: >98%) was synthesized by Blychem Ltd. (Billingham, UK). Collagenase H was purchased from Roche Diagnostics GmbH (Indianapolis, IN). Hank's balanced salt solution (HBSS) was purchased from Mediatech, Inc. (Manassas, VA). Ethyleneglycol-bis-aminoethylether-*N*,*N*,*N'*,*N'*-tetraacetic acid (EGTA), *S*-adenosyl-L-methionine (SAM), dimethyl sulfoxide (DMSO), and acetobromo-α-D-glucuronic acid methyl ester were purchased from Sigma-Aldrich (St. Louis, MO). *N*-2-hydroxy ethylpiperadine-*N'*-2-ethanosulfonic acid (HEPES) was purchased from Dojindo Laboratories (Kumamoto, Japan). Pooled human liver S9 from 15 donors was purchased from BD (Woburn, MA). All other chemicals and solvents were of analytical or high-performance liquid chromatography (HPLC) grade.

Synthesis of authentic standards of thiazolidinedione ring N-glucuronide M7 and thiazolidinedione ring-opened N-glucuronide M2.

The authentic standards of M7 and M2 were synthesized as outlined in Fig. 2, using the procedure described below.

Mass spectra were recorded using a JEOL JMS-700V, JEOL JMS-700QQ, or JEOL JMS-BU30 mass spectrometer (JEOL Ltd., Tokyo, Japan). Proton nuclear magnetic resonance (^{1}H NMR) spectra were recorded using a JEOL JNM-AL400 (JEOL Ltd.), VARIAN Mercury 400, or VARIAN Mercury 400Vx spectrometer

DMD Fast Forward. Published on February 25, 2010 as DOI: 10.1124/dmd.109.031583
This article has not been copyedited and formatted. The final version may differ from this version.

(Varian, Inc., Palo Alto, CA) and were reported in parts per million (δ) downfield from the internal standard tetramethylsilane (Me_4Si). All NMR spectra were consistent with the assigned structures. Column chromatography was performed by using Kishida reagent, silica gel SK-34 (Kishida Chemical Co., Ltd., Osaka, Japan) with solvents as described below. Thin-layer chromatography (TLC) analyses were performed with Merck reagent silica gel 60 F_{254} (0.25 mm thickness). Spots were visualized by either ultraviolet (UV) light or iodine.

3-((2R,3R,4S,5S,6S)-3,4,5-triacetoxy-6-methoxycarbonyl-tetrahydropyran-2-yl)-5-{4-[2-(5-ethyl-2-pyridinyl)ethoxy]benzyl}-thiazolidine-2,4-dione (2).

Acetobromo-α-D-glucuronic acid methyl ester (6.07 g, 15.3 mmol) was dissolved in acetonitrile (60 ml) and added to a solution containing pioglitazone hydrochloride (**1**; 3.00 g, 7.64 mmol), cesium carbonate (4.98 g, 15.3 mmol), and acetonitrile (90 ml) at 70°C (Baba and Yoshioka, 2007). The combined mixture was stirred for 3 h at 70°C. The reaction mixture was filtered with a silica gel short column (60 g, 70 × 300 mm; using a 1:1 by volume mixture of ethyl acetate and acetonitrile) and the filtrate was concentrated by evaporation under reduced pressure. The residue was purified by column chromatography with silica gel (300 g, 70 × 300 mm) using a gradient elution method, where a mixture of hexane and ethyl acetate (volume ratios ranging from 1:1 to 1:4, respectively) was used by increasing the percentage of ethyl acetate gradually, to give 4.27 g (6.35 mmol) of **2**: yield 83%; mass spectrometry (MS) *m/z* 673 $[M + H]^+$; ^1H NMR (400 MHz, $CDCl_3$) δ 1.24 (3H, t, J = 7.5 Hz, $PyCH_2CH_3$), 1.9–2.1 (9H, m, $OCOCH_3$), 2.63 (2H, q, J = 7.5 Hz, $PyCH_2CH_3$), 2.93 (1H, t, J = 12.7 Hz, $ArCH_2CH$), 3.22 (2H, dt, J = 3.2 and 9.5 Hz, $PyCH_2CH_2O$), 3.4–3.6 (1H, m,

DMD Fast Forward. Published on February 25, 2010 as DOI: 10.1124/dmd.109.031583
This article has not been copyedited and formatted. The final version may differ from this version.

ArC*H*$_2$CH), 3.75 (3H, d, *J* = 3.5 Hz, CO_2C*H*$_3$), 4.12 (1H, t, *J* = 7.2 Hz, C_5-*H*), 4.3–4.4 (3H, m, $PyCH_2C$*H*$_2$O, C_1-*H*), 5.3–5.4 (3H, m, C_2-*H*, C_3-*H*, C_4-*H*), 5.9–6.0 (1H, m, $ArCH_2C$*H*), 6.85 (2H, dd, *J* = 4.9 and 8.6 Hz, Ar-*H*), 7.10 (2H, dd, *J* = 1.6 and 8.6 Hz, Ar-*H*), 7.18 (1H, d, *J* = 7.8 Hz, Py-*H*), 7.45 (1H, dd, *J* = 1.9 and 7.8 Hz, Py-*H*), 8.39 (1H, d, *J* = 1.9 Hz, Py-*H*).

3-((2R,3R,4S,5S,6S)-6-allyloxycarbonyl-3,4,5-trihydroxy-tetrahydropyran-2-yl)-5-{4-[2-(5-ethyl-2-pyridinyl)ethoxy]benzyl}-thiazolidine-2,4-dione (3). A solution of **2** (4.26 g, 6.33 mmol), allyl alcohol (80 ml), and 4 N hydrogen chloride–dioxane (80 ml) was stirred for 4 h at room temperature and left standing for 3 days at room temperature. The reaction mixture was evaporated to dryness under reduced pressure. The residue was diluted with a 5:1 by volume mixture of methylene chloride and 2-propanol (150 ml), added to water (150 ml), and treated with 1 N NaOH solution until the aqueous layer was neutralized to pH 4. The organic layer was separated and the water layer was extracted with a 5:1 by volume mixture of methylene chloride and 2-propanol. The combined organic layers were washed with brine and dried over anhydrous sodium sulfate, after which the solvent was removed by evaporation under reduced pressure. The residue was purified by column chromatography with silica gel (200 g, 70 × 300 mm) using a gradient elution method, where a mixture of methylene chloride and methanol (volume ratios ranging from 30:1 to 10:1, respectively) was used by increasing the percentage of methanol gradually, to give 3.10 g (5.41 mmol) of **3**: yield 85%; MS *m/z* 573 $[M + H]^+$; ^{1}H NMR (400 MHz, $CDCl_3$) δ 1.24 (3H, dt, *J* = 3.8 and 10.7 Hz, $PyCH_2C$*H*$_3$), 2.62 (2H, q, *J* = 7.6 Hz, PyC*H*$_2CH_3$), 3.12 (1H, br s, ArC*H*$_2$CH), 3.1–3.3 (2H, m, PyC*H*$_2CH_2O$), 3.33 (1H, br s, ArC*H*$_2$CH),

DMD Fast Forward. Published on February 25, 2010 as DOI: 10.1124/dmd.109.031583
This article has not been copyedited and formatted. The final version may differ from this version.

3.4–4.0 (4H, m, C_2-*H*, C_3-*H*, C_4-*H*, C_5-*H*), 4.3–4.4 (2H, m, $PyCH_2CH_2O$), 4.4–4.5 (1H, m, C_1-*H*), 4.6–4.8 (2H, m, $OCH_2CH=CH_2$), 5.0–5.2 (1H, m, $ArCH_2CH$), 5.2–5.3 (1H, m, $OCH_2CH=CH_2$), 5.3–5.4 (1H, m, $OCH_2CH=CH_2$), 5.8–6.0 (1H, m, $OCH_2CH=CH_2$), 6.83 (2H, dd, *J* = 8.6 and 16.0 Hz, Ar-*H*), 7.11 (2H, dd, *J* = 8.6 and 21.9 Hz, Ar-*H*), 7.20 (1H, d, *J* = 7.8 Hz, Py-*H*), 7.48 (1H, dd, *J* = 1.8 and 7.8 Hz, Py-*H*), 8.3–8.4 (1H, m, Py-*H*).

3-((2R,3R,4S,5S,6S)-6-carboxy-3,4,5-trihydroxy-tetrahydropyran-2-yl)-5-{4-[2-(5-ethyl-2-pyridinyl)ethoxy]benzyl}-thiazolidine-2,4-dione (M7). A mixture of **3** (1.00 g, 1.75 mmol), morpholine (0.20 ml, 2.29 mmol), tetrakis(triphenylphosphine)palladium (0.40 g, 0.35 mmol), and methylene chloride (30 ml) was stirred for 4 h at room temperature. The reaction mixture was evaporated under reduced pressure. The residue was purified by column chromatography with silica gel (50 g, 70 × 300 mm) using a gradient elution method, where a mixture of ethyl acetate, methanol, and water (volume ratios ranging from 30:2:1 to 5:2:1, respectively) were used by increasing the percentage of methanol and water gradually, to give 0.60 g of yellow solid. This solid was purified using an SCL-10A HPLC system (Shimadzu Co. Kyoto, Japan). Separation was performed on an Inertosil ODS-3 column (50 × 500 mm, 5 μm; GL Sciences, Inc., Tokyo, Japan) and UV detection was carried out at 254 nm. The mobile phase, consisting of water containing 0.1% trifluoroacetic acid (TFA, solvent A) and acetonitrile (solvent B), was delivered at a flow rate of 50 ml/min. The gradient started at 10% solvent B and increased linearly to 35% solvent B for 60 min. The HPLC purification gave 0.53 g of TFA salt M7: yield 47%; MS *m/z* 533 $[M + H]^+$; MS/MS (product ions) *m/z* 134, 357; ^{1}H NMR (400 MHz, DMSO-d_6) δ 1.23 (3H, t, *J* =

DMD Fast Forward. Published on February 25, 2010 as DOI: 10.1124/dmd.109.031583
This article has not been copyedited and formatted. The final version may differ from this version.

7.5 Hz, $PyCH_2CH_3$), 2.73 (2H, q, *J* = 7.5 Hz, $PyCH_2CH_3$), 2.9–3.2 (1H, m, $ArCH_2CH$), 3.2–3.5 (5H, m, $PyCH_2CH_2O$, $ArCH_2CH$, C_3-*H*, C_4-*H*), 3.71 (1H, dd, *J* = 9.6 and 16.5 Hz, C_2-*H*), 4.0–4.3 (1H, m, C_5-*H*), 4.34 (2H, t, *J* = 6.1 Hz, $PyCH_2CH_2O$), 4.7–5.1 (2H, m, $ArCH_2CH$, C_1-*H*), 5.42 (3H, br s, O*H*), 6.8–6.9 (2H, m, Ar-*H*), 7.1–7.2 (2H, m, Ar-*H*), 7.79 (1H, dd, *J* = 1.7 and 8.2 Hz, Py-*H*), 8.19 (1H, d, *J* = 8.2 Hz, Py-*H*), 8.64 (1H, d, *J* = 1.7 Hz, Py-*H*), 12.9 (1H, br s, CO_2H).

(2S,3S,4S,5R,6R)-6-(1-carboxy-2-{4-[2-(5-ethyl-2-pyridinyl)ethoxy]phenyl}-ethylsulfanylcarbonylamino)-3,4,5-trihydroxy-tetrahydropyran-2-carboxylic acid (M2). A solution of M7 (1.00 g, 1.88 mmol), sodium acetate (2.00 g, 24.4 mmol), and 3:1 mixture of water and acetonitrile (20 ml) was stirred for 8 h at room temperature. The reaction mixture was left standing for 12 days at room temperature. The reaction mixture was acidified to pH 3 by the addition of TFA. This mixture was purified using an SCL-10A HPLC system. Separation was performed on an Inertosil ODS-3 column (50 × 500 mm, 5 μm) and UV detection was carried out at 254 nm. The mobile phase, consisting of water containing 0.1% TFA (solvent A) and acetonitrile (solvent B), was delivered at a flow rate of 50 ml/min. The gradient started at 10% solvent B and increased linearly to 30% solvent B for 60 min. The HPLC purification gave 0.48 g of TFA salt M2: yield 38%; MS *m/z* 551 $[M + H]^+$; MS/MS (product ions) *m/z* 134, 286, 332, 358, 375, 417; ^{1}H NMR (400 MHz, DMSO-d_6) δ 1.22 (3H, t, *J* = 7.6 Hz, $PyCH_2CH_3$), 2.74 (2H, q, *J* = 7.6 Hz, $PyCH_2CH_3$), 2.89 (1H, dd, *J* = 6.4 and 13.7 Hz, $ArCH_2CH$), 3.0–3.3 (3H, m, C_2-*H*, C_3-*H*, C_4-*H*), 3.15–3.25 (1H, m, $ArCH_2CH$), 3.34 (2H, t, *J* = 6.2 Hz, $PyCH_2CH_2O$), 3.62 (1H, d, *J* = 9.3 Hz, C_5-*H*), 4.09 (1H, dd, *J* = 6.4 and 8.8 Hz, $ArCH_2CH$), 4.34 (2H, t, *J* = 6.2 Hz, $PyCH_2CH_2O$), 4.7–4.8

DMD Fast Forward. Published on February 25, 2010 as DOI: 10.1124/dmd.109.031583
This article has not been copyedited and formatted. The final version may differ from this version.

(1H, m, C_1-*H*), 5.17 (3H, br s, O*H*), 6.84 (2H, d, *J* = 8.6 Hz, Ar-*H*), 7.11 (2H, d, *J* = 8.6 Hz, Ar-*H*), 7.80 (1H, d, *J* = 8.1 Hz, Py-*H*), 8.20 (1H, d, *J* = 8.1 Hz, Py-*H*), 8.65 (1H, d, *J* = 1.7 Hz, Py-*H*), 9.00 (1H, dd, *J* = 4.5 and 8.8 Hz, N*H*), 12.7 (2H, br s, CO_2*H*).

Preparation of freshly isolated human hepatocytes.

Human liver tissues from 3 donors were obtained from patients undergoing partial hepatectomy for metastatic liver tumors of colorectal cancer. Experimental procedures were performed according to the guidelines of the charitable state-controlled foundation, Human Tissue and Cell Research (HTCR, Regensburg, Germany), with informed patient's consent and approved by the local ethics committee of the University of Regensburg, Germany (Thasler et al., 2003). The liver samples were made anonymous. The human hepatocytes used were isolated and provided by Hepacult GmbH (Regensburg, Germany), after being commissioned by HTCR and Daiichi Sankyo Europe GmbH (Martinsried, Germany). Cells were isolated using a modified two-step EGTA-collagenase perfusion procedure (Weiss et al., 2003). The human hepatocytes were washed twice with HBSS and suspended in HBSS at a viable cell density of 2×10^6 cells/ml. As determined by the trypan blue dye exclusion method, the cellular viabilities of the human hepatocytes were 66, 73, and 81%.

Preparation of freshly isolated rat and monkey hepatocytes.

All experimental procedures were performed in accordance with the in-house guidance of the Institutional Animal Care and Use Committee of Daiichi Sankyo Co., Ltd. Freshly isolated rat and monkey hepatocytes were obtained by the standard

DMD Fast Forward. Published on February 25, 2010 as DOI: 10.1124/dmd.109.031583
This article has not been copyedited and formatted. The final version may differ from this version.

method (Moldeus et al., 1978). The rat hepatocytes were prepared from a male Sprague-Dawley rat (Crl:CD, 7 weeks old, body weight: 170 g). The rat hepatocytes were washed twice with HBSS and suspended in HBSS at a viable cell density of 2×10^6 cells/ml. The cellular viability of the rat hepatocytes was 93%, as determined by the trypan blue dye exclusion method. The monkey hepatocytes were prepared from 2 male cynomolgus monkeys (*Macaca fasicularis*, 5 years old as the estimated age). The monkey hepatocytes were washed twice with HBSS and suspended in HBSS at a viable cell density of 2×10^6 cells/ml. As determined by the trypan blue dye exclusion method, the cellular viabilities of the monkey hepatocytes were 91 and 94%.

Incubation of [^{14}C]pioglitazone with freshly isolated human, rat, and monkey hepatocytes.

[^{14}C]pioglitazone (30 μM) was incubated with viable human, rat, or monkey hepatocytes suspended with HBSS (2×10^6 cells/ml) for 3 h at 37°C under 95 % O_2 and 5% CO_2 in an incubator (incubation volume: 2.5 ml each; incubation numbers for humans: n = 3, rat: n = 1, monkeys: n = 2, as collected in the above section). For human hepatocytes, the initial viabilities were 66–81% and the remaining CYP3A4 activities (testosterone 6β-hydroxylation) after incubation for 3 h were 60–100% of the initial activity. For rat and monkey hepatocytes, the initial viabilities were 93% and 91–94%, respectively. The reactions were terminated by the addition of acetonitrile (5 ml). The cells homogenized by sonication and the samples of the incubated hepatocytes were stored at approximately –80°C until use. For each species (humans, rat, or monkeys), the samples were pooled and centrifuged at 21,600 *g* for 5 min at 4°C (himac CF15D; Hitachi Koki Co., Ltd., Tokyo, Japan) and each supernatant was

carefully collected. Each supernatant was evaporated under a nitrogen stream to an approximate final volume of 1.5 ml. Each concentrated sample was used for the analysis of the metabolites by radioactivity detection-HPLC (radio-HPLC), LC/MS, and LC/MS/MS.

Incubation of M7 with human liver S9.

Incubation of M7 **(**authentic standard) with pooled human liver S9 was performed as follows. The incubation mixture contained 10 μM M7 (dissolved in methanol) and 1 mg/ml protein from human liver S9 in 500 μl of 50 mM potassium phosphate (pH 7.4) in the presence or absence of 2 mM SAM. The incubations were carried out for 2 h at 37°C in a shaking water bath. Control incubation without human liver S9 and with SAM alone was carried out under otherwise similar conditions. Of the 500 μl incubation outtake, 50 μl aliquots were taken and quenched by adding acetonitrile (100 μl). After centrifugation at 21,600 *g* for 5 min at 4°C, the supernatant was collected and diluted with 50 μl of water and analyzed by LC/MS and LC/MS/MS.

Radio-HPLC analysis.

Samples from the hepatocyte incubations were analyzed by radio-HPLC. The radio-HPLC analysis was conducted using an L-6000 HPLC system (Hitachi, Ltd., Tokyo, Japan) combined with a radiomatic 525TR radioactivity detector (PerkinElmer Life and Analytical Sciences, Boston, MA). Chromatographic separation was performed on a YMC-Pack ODS-A column (6.0 × 150 mm, 5 μm; YMC Co., Ltd., Kyoto, Japan) at ambient temperature. The mobile phase, consisting of water containing 0.01% TFA (solvent A) and acetonitrile containing 0.01% TFA (solvent B),

DMD Fast Forward. Published on February 25, 2010 as DOI: 10.1124/dmd.109.031583
This article has not been copyedited and formatted. The final version may differ from this version.

was delivered at a flow rate of 1 ml/min. The gradient started at 15% solvent B, increased linearly to 50% solvent B for 30 min, increased linearly to 90% solvent B for 5 min, and then held at 90% solvent B for 5 min. The column effluent was monitored using an L-4000 UV detector (UV at 225 nm; Hitachi, Ltd.) and a radioactivity detector with a 3 ml/min flow rate for the Ultima-Flo M liquid scintillator (PerkinElmer Life and Analytical Sciences).

LC/MS and LC/MS/MS analyses.

The conditions described below were used for the LC/MS and LC/MS/MS analyses of pioglitazone metabolites formed during incubation with human, rat, and monkey hepatocytes. These analyses were performed using a Q-Tof mass spectrometer (Waters, Manchester, UK) with an L-7000 HPLC system (Hitachi, Ltd.) consisting of an intelligent pump (model L-7100), a column oven (model L-7300), a chromato-integrator (model D-7500), and a UV detector (model L-7400S). The LC/MS analysis was conducted using electrospray ionization (ESI) in the positive ion mode. The capillary voltage and cone voltage were set at 3300 V and 45 V, respectively. The source temperature and desolvation gas temperature were 120°C and 300°C, respectively. The mass range from *m/z* 50 to 1000 was acquired with an integration time of 1 sec. The LC/MS/MS analyses were performed using a collision energy of 20 eV and xenon as the collision gas. Chromatographic separation was performed on a YMC-Pack ODS-A column (1.5 × 150 mm, 5 μm); the column temperature was maintained at 30°C, and UV detection was carried out at 225 nm. The mobile phase consisted of water containing 0.01% TFA (solvent A) and acetonitrile containing 0.01% TFA (solvent B). The gradient started at 15% solvent B,

increased linearly to 50% solvent B for 30 min, increased linearly to 90% solvent B for 5 min, and was then held at 90% solvent B for 5 min. The flow rate was set at 0.1 ml/min and the elution flow from HPLC was introduced into the Q-Tof mass spectrometer ionization source through an ESI interface.

The conditions described below were used for the LC/MS and LC/MS/MS analyses of the generated products of M7 in human liver S9. These analyses were performed using a Waters Q-Tof Premier mass spectrometter (Waters, Manchester, UK) with a Waters ACQUITY UPLC system (Waters, Milford, MA) consisting of a binary solvent manager, a sample manager, a photodiode array (PDA) detector, and a column heater. The LC/MS analysis was conducted using ESI in the positive ion mode. The capillary voltage and cone voltage were set at 3300 V and 40 V, respectively. The source temperature and desolvation gas temperature were 120°C and 300°C, respectively. The mass range from *m/z* 50 to 1000 was acquired with an integration time of 0.5 sec. The LC/MS/MS analysis was performed using a collision energy of 25 eV and argon as the collision gas. Chromatographic separation was performed on a YMC-UltraHT Pro C18 column (2.0 × 50 mm, 2 μm); the column temperature was maintained at 40°C, and UV detection was carried out at 225 nm. The mobile phase consisted of water containing 0.01% TFA (solvent A) and acetonitrile containing 0.01% TFA (solvent B). The gradient started at 10% solvent B and increased linearly to 20% solvent B for 9 min. The flow rate was set at 0.2 ml/min, and the elution flow from UPLC was introduced into the Q-Tof ionization source through an ESI interface.

DMD Fast Forward. Published on February 25, 2010 as DOI: 10.1124/dmd.109.031583
This article has not been copyedited and formatted. The final version may differ from this version.

Results

Metabolic profiles of pioglitazone in freshly isolated human, rat, and monkey hepatocytes.

Representative radiochromatograms after incubation of [^{14}C]pioglitazone with freshly isolated human, rat, and monkey hepatocytes are shown in Fig. 3. Thirteen metabolites peaks in human hepatocytes were detected and designated as M1–M13 according to their order of retention time in HPLC. An identical set of metabolites (M1–M13) was also detected in monkey hepatocytes. In rat hepatocytes, M1–M3, M5–M7, M9–M11, and M13 were also detected. M4, M8, and M12 were not detected in rat hepatocytes in this study. M1, M2, M3, M7, M8, and M11 were novel metabolites of pioglitazone, while M4, M5, M6, M9, M10, M12, and M13 were previously reported metabolites as M-VI, M-IV, M-V, M-VII, M-II, M-IX, and M-III, respectively (Krieter et al., 1994; Kiyota et al., 1997; Maeshiba et al., 1997; Shen et al., 2003) (Table 1).

Structure analysis of M8.

The positive ion LC/MS spectrum of M8 showed a protonated molecule $[M + H]^+$ at *m/z* 345. The positive ion LC/MS/MS spectrum of the precursor ion $[M + H]^+$ at *m/z* 345 and the proposed fragmentation scheme of M8 are shown in Fig. 4. Product ions at *m/z* 119, 134, 240, 254, 280, and 328 were obtained. The most intense product ion at *m/z* 134 was formed via the loss of 211 Da from the ion $[M + H]^+$ at *m/z* 345. The product ions at *m/z* 119 and 134 indicated that the 2-(5-ethyl-2-pyridine)ethyl moiety was not modified. On the other hand, the product ions at *m/z* 254, 280, and

DMD Fast Forward. Published on February 25, 2010 as DOI: 10.1124/dmd.109.031583
This article has not been copyedited and formatted. The final version may differ from this version.

328 from the ion $[M + H]^+$ at *m/z* 345 suggested a thiazolidinedione ring metabolism. The product ion at *m/z* 254 was formed via the elimination of the methylmercapto and the amide groups from the ion $[M + H]^+$ at *m/z* 345. Based on these results, M8 was proposed to be a thiazolidinedione ring-opened methylmercapto amide (Fig. 4).

Structure analysis of M1.

The positive ion LC/MS spectrum of M1 showed a protonated molecule $[M + H]^+$ at *m/z* 361, which was 16 Da higher than that of M8. The positive ion LC/MS/MS spectrum of M1, which was obtained by collision-induced dissociation (CID) of the ion $[M + H]^+$ at *m/z* 361, and the proposed fragmentation scheme are shown in Fig. 5. Product ions at *m/z* 119, 134, 254, 280, and 297 were obtained. The most intense product ion at *m/z* 254 was formed via the loss of 107 Da from the ion $[M + H]^+$ at *m/z* 361. The product ions at *m/z* 119 and 134 indicated that the 2-(5-ethyl-2-pyridine)ethyl moiety was not modified. On the other hand, the product ions at *m/z* 254, 280, and 297 provided strong evidence for metabolic transformation of the thiazolidinedione ring. The product ion at *m/z* 297 was formed via the elimination of the methyl sulfoxide group from the ion $[M + H]^+$ at *m/z* 361. The product ion at *m/z* 254 was formed via the elimination of the methyl sulfoxide and the amide groups from the ion $[M + H]^+$ at *m/z* 361. Based on these results, M1 was proposed to be a thiazolidinedione ring-opened methyl sulfoxide amide produced by the oxidation of the sulfur atom of M8 (Fig. 5).

Structure analysis of M3.

The positive ion LC/MS spectrum of M3 showed a protonated molecule $[M + H]^+$

at *m/z* 377, which was 16 Da higher than that of M1. The positive ion LC/MS/MS spectrum of the precursor ion $[M + H]^+$ at *m/z* 377 and the proposed fragmentation scheme of M3 are shown in Fig. 6. Product ions at *m/z* 119, 134, 254, 280, and 297 were obtained. The most intense product ion at *m/z* 254 was formed via the loss of 123 Da from the ion $[M + H]^+$ at *m/z* 377. The product ions at *m/z* 119 and 134 indicated that the 2-(5-ethyl-2-pyridine)ethyl moiety was not modified. On the other hand, the product ions at *m/z* 254, 280, and 297 from the ion $[M + H]^+$ at *m/z* 377 suggested a thiazolidinedione ring metabolism. The product ion at *m/z* 297 was formed via the elimination of the methyl sulfone group from the ion $[M + H]^+$ at *m/z* 377. The product ion at *m/z* 254 was formed via the elimination of the methyl sulfone and the amide groups from the ion $[M + H]^+$ at *m/z* 377. Based on these results, M3 was proposed to be a thiazolidinedione ring-opened methyl sulfone amide produced by further oxidation of the sulfur atom of the metabolite M1 (Fig. 6).

Structure analysis of M7.

The positive ion LC/MS spectrum of M7 showed a protonated molecule $[M + H]^+$ at *m/z* 533. The positive ion LC/MS/MS spectrum of the precursor ion $[M + H]^+$ at *m/z* 533 and the proposed fragmentation scheme of M7 are shown in Fig. 7. Product ions at *m/z* 134 and 357 were obtained. The most intense product ion at *m/z* 357 was formed via the loss of 176 Da from the ion $[M + H]^+$ at *m/z* 533, corresponding to the glucuronic acid moiety. The product ion at *m/z* 134 was formed via the elimination of the 2-(5-ethyl-2-pyridine)ethyl moiety from the ion at *m/z* 357. Furthermore, the positive ion LC/MS/MS spectrum (Fig. 7a) and HPLC retention time (Fig. 7b) of M7 were identical to those of the authentic standard M7 (Figs. 7c and 7d). Based on

DMD Fast Forward. Published on February 25, 2010 as DOI: 10.1124/dmd.109.031583
This article has not been copyedited and formatted. The final version may differ from this version.

these results, M7 was identified as a thiazolidinedione ring *N*-glucuronide (Fig. 7e).

Structure analysis of M2.

The positive ion LC/MS spectrum of M2 showed a protonated molecule $[M + H]^+$ at *m/z* 551, which was 18 Da higher than that of the thiazolidinedione ring *N*-glucuronide M7. The positive ion LC/MS/MS spectrum of the ion $[M + H]^+$ at *m/z* 551 and the proposed fragmentation scheme of M2 are shown in Fig. 8. Product ions at *m/z* 134, 286, 332, 358, 375, and 417 were obtained. The product ion at *m/z* 375 was formed via the loss of 176 Da from the ion $[M + H]^+$ at *m/z* 551, corresponding to the glucuronic acid moiety. Therefore, it was suggested that M2 was a glucuronide metabolite. The product ion at *m/z* 417 was formed via the elimination of a part of the glucuronic acid moiety from the ion $[M + H]^+$ at *m/z* 551. The product ions at *m/z* 286, 332, and 358 suggested a thiazolidinedione ring metabolism. Furthermore, the positive ion LC/MS/MS spectrum (Fig. 8a) and HPLC retention time (Fig. 8b) of M2 were identical to those of the authentic standard M2 (Figs. 8c and 8d). Based on these results, M2 was identified as a thiazolidinedione ring-opened *N*-glucuronide, a hydrolyzed metabolite of the thiazolidinedione ring *N*-glucuronide M7 (Fig. 8e).

Structure analysis of M11.

The positive ion LC/MS spectrum of M11 showed a protonated molecule $[M + H]^+$ at *m/z* 346. The positive ion LC/MS/MS spectrum of the precursor ion $[M + H]^+$ at *m/z* 346 and the proposed fragmentation scheme of M11 are shown in Fig. 9. Product ions at *m/z* 119, 134, 254, 270, and 286 were obtained. The most intense product ion at *m/z* 134 was formed via the loss of 212 Da from the ion $[M + H]^+$ at *m/z*

DMD Fast Forward. Published on February 25, 2010 as DOI: 10.1124/dmd.109.031583
This article has not been copyedited and formatted. The final version may differ from this version.

346. The product ions at *m/z* 119 and 134 indicated that the 2-(5-ethyl-2-pyridine)ethyl moiety was not modified. On the other hand, the product ions at *m/z* 254 and 286 from the ion $[M + H]^+$ at *m/z* 346 suggested a thiazolidinedione ring metabolism. The product ion at *m/z* 286 was formed via the elimination of the methyl and the carboxylic acid groups from the ion $[M + H]^+$ at *m/z* 346. The product ion at *m/z* 254 was formed via the elimination of the methylmercapto and the carboxylic acid groups from the ion $[M + H]^+$ at *m/z* 346. Based on these results, M11 was proposed to be a thiazolidinedione ring-opened methylmercapto carboxylic acid (Fig. 9).

Metabolism of M7 in human liver S9.

The metabolism of M7 was studied using human liver S9. Incubation of M7 with human liver S9 in the presence of SAM yielded a thiazolidinedione ring-opened *N*-glucuronide M2, a newly generated product in human liver S9 (S9P1), and a thiazolidinedione ring-opened methylmercapto carboxylic acid M11 (Fig. 10). Incubation of M7 with human liver S9 in the absence of SAM yielded M2 and S9P1 (data not shown). M2 and S9P1 also resulted from incubation of M7 without human liver S9 and with SAM alone (data not shown).

Structure analysis of S9P1.

The positive ion LC/MS spectrum of S9P1 showed a protonated molecule $[M + H]^+$ at *m/z* 332. The positive ion LC/MS/MS spectrum of the precursor ion $[M + H]^+$ at *m/z* 332 and the proposed fragmentation scheme of S9P1 are shown in Fig. 11. Product ions at *m/z* 119, 134, 254, 270, and 286 were obtained. The most intense

DMD Fast Forward. Published on February 25, 2010 as DOI: 10.1124/dmd.109.031583
This article has not been copyedited and formatted. The final version may differ from this version.

product ion at *m/z* 134 was formed via the loss of 198 Da from the ion $[M + H]^+$ at *m/z* 332. The product ions at *m/z* 119 and 134 indicated that the 2-(5-ethyl-2-pyridine)ethyl moiety was not modified. On the other hand, the product ions at *m/z* 254 and 286 from the ion $[M + H]^+$ at *m/z* 332 suggested thiazolidinedione ring metabolism. The product ion at *m/z* 286 was formed via the elimination of the carboxylic acid group from the ion $[M + H]^+$ at *m/z* 332. The product ion at *m/z* 254 was formed via the elimination of the mercapto and the carboxylic acid groups from the ion $[M + H]^+$ at *m/z* 332. Based on these results, S9P1 was proposed to be a thiazolidinedione ring-opened mercapto carboxylic acid (Fig. 11).

Discussion

In this study, we detected thirteen metabolites (M1–M13) in an in vitro metabolic system of pioglitazone with freshly isolated human, rat, and monkey hepatocytes, and their structures were elucidated by LC/MS/MS. Furthermore, metabolites M2, S9P1, and M11 were detected in an in vitro metabolic system with human liver S9 using M7 (authentic standard) as a substrate. Based on the structures of the elucidated metabolites, the in vitro metabolic pathways for pioglitazone are proposed, as shown in Fig. 12.

Novel metabolic pathways for pioglitazone, *N*-glucuronidation of the thiazolidinedione ring of pioglitazone to form M7 and hydrolysis of M7 to form M2, were observed in hepatocytes. As a result of the presence of these metabolites, the metabolic pathway via the thiazolidinedione ring *N*-glucuronide M7 and subsequent hydrolysis to the thiazolidinedione ring-opened *N*-glucuronide M2 is proposed. This thiazolidinedione ring opening pathway is distinct from the known oxidative thiazolidinedione ring opening pathway for troglitazone (Kassahun et al., 2001) and pioglitazone (Baughman et al., 2005). Baughman group has investigated the metabolites related to reactive metabolite formation using non-labeled pioglitazone (10 μM) in freshly isolated human hepatocytes by the detection method of a generic neutral loss method of 129 amu. However, they have not found *N*-glucuronide of pioglitazone. On the other hand, we have focused on the exhaustive investigation to find minor metabolites in freshly isolated hepatocytes using [^{14}C]pioglitazone (30 μM).

Moreover, in the human liver S9 study using M7, we inferred that M7 is metabolized to S9P1 via M2 and consequent *S*-methylation to M11 immediately in the

presence of SAM. These are also novel metabolic pathways for pioglitazone. We have recently reported similar metabolic pathways in another thiazolidinedione ring-containing drug, rosiglitazone (Uchiyama et al., 2010). Thus, the metabolic pathways of ring opening via *N*-glucuronidation of the thiazolidinedione ring are assumed to be common metabolic reactions to the thiazolidinedione ring.

As examples of *N*-glucuronidation to analogs related to thiazolidinediones, *N*-glucuronides of MaxiPost (BMS-204352) (Zhang et al., 2005), Bucolome (Mohri et al., 1985), 5-ethyl-5-phenylhydantoin (Nirvanol) (Maguire et al., 1982) for *N*-glucuonidation of cyclic amide compounds, and that of PNU-107859 for *N*-glucuonidation of cyclic thioamide compound (Kuo et al., 1999) have been reported. For all cases, *N*-glucuronides were found to be major metabolites and stable. The non-enzymatic hydrolysis of synthetic M7 to M2 was observed (half-life of about 0.7 h) in buffer solution (pH 7.4) during incubation at 37°C (data not shown). The chemical mechanism of ring-opening of thiazolidinedione of pioglitazone is unknown. However, after *N*-glucuronidation of the thiazolidinedione ring, the formation of hydrogen bonding between the hydroxyl group at 2-position of the glucuronic acid moiety and the carbonyl group at 4-position of the thiazolidinedione ring would be proposed. As a result, the thiazolidinedione ring may increase electrophilicity, become to be easily attacked by nucleophile and hydrolyzed. In addition, if the chemical reactivity of M7 is very high, there is the possibility of detecting glutathione conjugates, but no glutathione conjugates were observed in this study.

The known oxidative thiazolidinedione ring opening and subsequent pathways via reactive intermediates generation of troglitazone have been proposed on the basis of identification of glutathione conjugate metabolites using human liver microsomes and

DMD Fast Forward. Published on February 25, 2010 as DOI: 10.1124/dmd.109.031583
This article has not been copyedited and formatted. The final version may differ from this version.

cDNA-expressed cytochrome P450 isoforms (Kassahun et al., 2001). Similar metabolic pathways have been reported for pioglitazone (Baughman et al., 2005) and the thiazolidinedione derivatives MK-0767 (Karanam et al., 2004; Liu et al., 2004; Kochnsky et al., 2006) and MRL-A (Reddy et al., 2005). In this study, we have identified M8, M1, and M3 as new metabolites of pioglitazone via the thiazolidinedione ring-opened mercapto amide. We estimate that these metabolites are sequentially generated by the oxidative thiazolidinedione ring opening and subsequent pathways, which agree well with the previous proposed metabolic activation scheme of pioglitazone (Baughman et al., 2005).

Besides those described above, the known metabolic pathways for pioglitazone (Krieter et al., 1994; Kiyota et al., 1997; Maeshiba et al., 1997; Shen et al., 2003) were also confirmed in this study: the generation of M4 (M-VI), M5 (M-IV), M6 (M-V), M9 (M-VII), M10 (M-II), M12 (M-IX), and M13 (M-III). Thus, since these known metabolites observed in vivo have been determined in this study, these hepatocytes systems seem to reflect the in vivo metabolism of pioglitazone. However, since the ratios of the peak area of M7 and M2 to M5, a major metabolite in Fig. 3, were 0.06 and 0.12 for human hepatocytes, there may be a low amount of these metabolites formed in vivo.

Some toxicological concerns have been expressed regarding the oxidative thiazolidinedione ring opening reaction of thiazolidinedione-containing drugs (Kassahun et al., 2001; Tettey et al., 2001; Smith, 2003; He et al., 2004; Baughman et al., 2005; Alvarez-Sanchez et al., 2006). For this new ring opening reaction via *N*-glucuonidation of pioglitazone, further studies are needed to investigate the toxicological evaluation.

DMD Fast Forward. Published on February 25, 2010 as DOI: 10.1124/dmd.109.031583
This article has not been copyedited and formatted. The final version may differ from this version.

Acknowledgements

We thank Dr. Osamu Okazaki, Drug Metabolism and Pharmacokinetics Research Laboratories, Daiichi Sankyo Co., Ltd., for his careful reading of the document and his scientific expertise.

References

Alvarez-Sanchez R, Montavon F, Hartung T, and Pahler A (2006) Thiazolidinedione bioactivation: a comparison of the bioactivation potentials of troglitazone, rosiglitazone, and pioglitazone using stable isotope-labeled analogues and liquid chromatography tandem mass spectrometry. *Chem Res Toxicol* **19:**1106-1116.

Baba A and Yoshioka T (2007) An improved chemo-enzymatic synthesis of 1-β-*O*-acyl glucuronides: higly chemoselective enzymatic removal of protecting groups from corresponding methyl acetyl derivatives. *J Org Chem* **72:**9541-9549.

Baba S (2001) Pioglitazone: a review of Japanese clinical studies. *Curr Med Res Opin* **17:**166-189.

Baughman TM, Graham RA, Wells-Knecht K, Silver IS, Tyler LO, Wells-Knecht M, and Zhao Z (2005) Metabolic activation of pioglitazone identified from rat and human liver microsomes and freshly isolated hepatocytes. *Drug Metab Dispos* **33:**733-738.

Chilcott J, Tappenden P, Jones ML, and Wight JP (2001) A systematic review of the clinical effectiveness of pioglitazone in the treatment of type 2 diabetes mellitus. *Clin Ther* **23:**1792-1823.

Eckland DA and Danhof M (2000) Clinical pharmacokinetics of pioglitazone. *Exp Clin Endocrinol Diabetes* **108 (suppl 2) :**234-242.

Gale EAM (2001) Lessons from the glitazone: a story of drug development. *Lancet* **357:**1870-1875.

Graham DJ, Green L, Senior JR, and Nourjah P (2003) Troglitazone-induced liver failure: a case study. *Am J Med* **114:**299-306.

He K, Talaat RE, Pool WF, Reily MD, Reed JE, Bridges AJ, and Woolf TF (2004) Metabolic activation of troglitazone: identification of a reactive metabolite and mechanisms involved. *Drug Metab Dispos* **3**2**:**639-646.

Jaakkola T, Laitila J, Neuvonen PJ, and Backman JT (2006) Pioglitazone is metabolised by CYP2C8 and CYP3A4 in vitro: potential for interactions with CYP2C8 inhibitors. *Basic Clin Pharmacol Toxicol* **99:**44-51.

Karanam BV, Hop CECA, Liu DQ, Wallace M, Dean D, Satoh H, Komuro M, Awano K, and Vincent SH (2004) In vitro metabolism of MK-0767 [(±)-5-[(2,4-dioxothiazolidin-5-yl)methyl]-2-methoxy-*N*-[[(4-trifluoromethyl) phenyl]methyl]benzamide], a peroxisome proliferator-activated receptor α/γ agonist. I. Role of cytochrome P450, methyltransferases, flavin monooxygenases, and esterases. *Drug Metab Dispos* **32:**1015-1022.

Kassahun K, Pearson PG, Tang W, McIntosh I, Leung K, Elmore C, Dean D, Wang R, Doss G, and Baillie TA (2001) Studies on the metabolism of troglitazone to reactive intermediates in vitro and in vivo. Evidence for novel biotransformation pathways

involving quinone methide formation and thiazolidinedione ring scission. *Chem Res Toxicol* **14:**62-70.

Kiyota Y, Kondo T, Maeshiba Y, Hashimoto A, Yamashita K, Yoshimura Y, Motohashi M, and Tanayama S (1997) Studies on the metabolism of the new antidiabetic agent pioglitazone. Identification of metabolites in rats and dogs. *Arzneim-Forsch/Drug Res* **47:**22-28.

Kochansky CJ, Rippley RK, Yan KX, Song H, Wallace MA, Dean D, Jones AN, Lasseter K, Schwartz J, Vincent SH, Franklin RB, and Wagner J (2006) Absorption, metabolism, and excretion of [^{14}C]MK-0767 (2-methoxy-5-(2,4-dioxo-5-thiazolidinyl)-*N*-[[4-(trifluoromethyl)phenyl] methyl]benzamide) in humans. *Drug Metab Dispos* **34:**1457-1461.

Krieter PA, Colletti AE, Doss GA, and Miller RR (1994) Disposition and metabolism of the hypoglycemic agent pioglitazone in rats. *Drug Metab Dispos* **22:**625-630.

Kuo MS, Yurek DA, Mizsak SA, Prairie MD, Mattern SJ, and DeKoning TF (1999) Isolation and identification of a major metabolite of PNU-107859, an MMP inhibitor from the biliary fluid of rats. *J Pharm Sci* **88:**705-708.

Liu DQ, Karanam BV, Doss GA, Sidler RR, Vincent SH, and Hop CECA (2004) In vitro metabolism of MK-0767 [(±)-5-[(2,4-dioxothiazolidin-5-yl)methyl]-2-methoxy-*N*-[[(4-trifluoromethyl)-phenyl]

methyl]benzamide], a peroxisome proliferator-activated receptor α/γ agonist. II. Identification of metabolites by liquid chromatography-tandem mass spectrometry. *Drug Metab Dispos* **32:**1023-1031.

Maeshiba Y, Kiyota Y, Yamashita K, Yoshimura Y, Motohashi M, and Tanayama S (1997) Disposition of the new antidiabetic agent pioglitazone in rats, dogs, and monkeys. *Arzneim-Forsch/Drug Res* **47:**29-35.

Maguire JH, Butler TC, and Dudley KH (1982) 5-ethyl-5-phenylhydantoin N-glucuronide, the major urinary metabolite of 5-ethyl-5-phenylhydantoin (Nirvanol) in the dog. *Drug Metab Dispos* **10:**595-598.

Mohri K, Uesugi T, and Kamisaka K (1985) Bucolome *N*-glucuronide: purification and identification of a major metabolite of bucolome in rat bile. *Xenobiotica* **15:**615-621.

Moldeus P, Hogberg J, and Orrenius S (1978) Isolation and use of liver cells. *Methods Enzymol* **52:**60-71.

Muschler E, Lal J, Jetter A, Rattay A, Zanger U, Zadoyan G, Fuhr U, and Kirchheiner J (2009) The role of human CYP2C8 and CYP2C9 variants in pioglitazone metabolism in vitro. *Basic Clin Pharmacol Toxicol* **105:**374-379.

Reddy VBG, Karanam BV, Gruber WL, Wallace MA, Vincent SH, Franklin RB, and Baillie TA (2005) Mechanistic studies on the metabolic scission of thiazolidinedione derivatives to acyclic thiols. *Chem Res Toxicol* **18:**880-888.

Shen Z, Reed JR, Creighton M, Liu DQ, Tang YS, Hora DF, Feeney W, Szewczyk J, Bakhtiar R, Franklin RB, and Vincent SH (2003) Identification of novel metabolites of pioglitazone in rat and dog. *Xenobiotica* **33:**499-509.

Smith MT (2003) Mechanisms of troglitazone hepatotoxicity. *Chem Res Toxicol* **16:**679-687.

Sood V, Colleran K, and Burge MR (2000) Thiazolidinediones: a comparative review of approved uses. *Diabetes Technol Ther* **2:**429-440.

Tettey JN, Maggs JL, Rapeport WG, Pirmohamed M, and Park BK (2001) Enzyme-induction dependent bioactivation of troglitazone and troglitazone quinone in vivo. *Chem Res Toxicol* **14:**965-974.

Thasler WE, Weiss TS, Schillhorn K, Stoll P-T, Irrgang B, and Jauch K-W (2003) Charitable state-controlled foundation human tissue and cell research: ethic and legal aspects in the supply of surgically removed human tissue for research in the academic and commercial sector in germany. *Cell Tissue Bank* **4:**49-56

Uchiyama M, Oguchi M, Yamamura N, koda H, Fischer T, Mueller J, Izumi T, and Iwabuchi H (2010) Identification of novel metabolites of rosiglitazone in freshly isolated human, rat, and monkey hepatocytes by liquid chromatography/tandem mass spectrometry. *J Mass Spectrom Soc Jap* **58:**1-11.

Weiss TS, Pahernik S, Scheruebl I, Jauch K-W, and Thasler WE (2003) Cellular damage to human hepatocytes through repeated application of 5-aminolevulinic acid. *J Hepatol* **38:**476-482.

Yamamoto Y, Yamazaki H, Ikeda T, Watanabe T, Iwabuchi H, Nakajima M, and Yokoi T (2002) Formation of a novel quinone epoxide metabolite of troglitazone with cytotoxic to HepG2 cells. *Drug Metab Dispos* **30:**155-160.

Zhang D, Krishna R, Wang L, Zeng J, Mitroka J, Dai R, Narasimhan N, Reeves RA, Srinivas NR, and Klunk LJ (2005) Metabolism, pharmacokinetics, and protein covalent binding of radiolabeled MaxiPost (BMS-204352) in humans. *Drug Metab Dispos* **33:**83-93.

DMD Fast Forward. Published on February 25, 2010 as DOI: 10.1124/dmd.109.031583
This article has not been copyedited and formatted. The final version may differ from this version.

Footnotes

a) Send reprint requests to Minoru Uchiyama, Drug Metabolism & Pharmacokinetics Laboratories, R&D Division, Daiichi Sankyo Co., Ltd., 1-2-58, Hiromachi, Shinagawa-ku, Tokyo 140-8710, Japan. Phone: +81-3-3492-3131; Fax: +81-3-5436-8567; E-mail:

Figure Legends

Figure 1 Chemical structure of [^{14}C]pioglitazone.

Figure 2 Synthetic scheme of thiazolidinedione ring *N*-glucuronide M7 and thiazolidinedione ring-opened *N*-glucuronide M2.

Figure 3 Representative radiochromatograms after incubation of [^{14}C]pioglitazone with freshly isolated human, rat, and monkey hepatocytes. [^{14}C]pioglitazone (30 μM) was incubated with freshly isolated human, rat, and monkey hepatocytes for 3 h at 37° C. Radio-HPLC analysis was conducted as described in *Materials and Methods.*

Figure 4 Positive ion LC/MS/MS spectrum of the ion $[M + H]^+$ at *m/z* 345 and the proposed fragmentation scheme of M8.

Figure 5 Positive ion LC/MS/MS spectrum of the ion $[M + H]^+$ at *m/z* 361 and the proposed fragmentation scheme of M1.

Figure 6 Positive ion LC/MS/MS spectrum of the ion $[M + H]^+$ at *m/z* 377 and the proposed fragmentation scheme of M3.

Figure 7 Mass spectrometric comparison of M7 and the authentic standard M7: (a) positive ion LC/MS/MS spectrum of M7, (b) extracted ion chromatogram of the ion $[M + H]^+$ at *m/z* 533 of M7, (c) positive ion LC/MS/MS spectrum of authentic standard M7, (d) extracted ion chromatogram of the ion $[M + H]^+$ at *m/z* 533 of the authentic standard M7, and (e) the proposed fragmentation scheme of M7.

Figure 8 Mass spectrometric comparison of M2 and the authentic standard M2: (a) positive ion LC/MS/MS spectrum of M2, (b) extracted ion chromatogram of the ion $[M + H]^+$ at *m/z* 551 of M2, (c) positive ion LC/MS/MS spectrum of authentic standard M2, (d) extracted ion chromatogram of the ion $[M + H]^+$ at *m/z* 551 of the authentic

standard M2, and (e) the proposed fragmentation scheme of M2.

Figure 9 Positive ion LC/MS/MS spectrum of the ion $[M + H]^+$ at *m/z* 346 and the proposed fragmentation scheme of M11.

Figure 10 Extracted ion chromatograms of the metabolites after incubation of M7 with human liver S9 in the presence of SAM. (a) $[M + H]^+$ at *m/z* 551 of thiazolidinedione ring-opened *N*-glucuronide M2, (b) $[M + H]^+$ at 332 of S9P1, and (c) $[M + H]^+$ at *m/z* 346 of thiazolidinedione ring-opened methylmercapto carboxylic acid M11. Positive ion LC/MS analysis was conducted as described in *Materials and Methods.*

Figure 11 Positive ion LC/MS/MS spectrum of the ion $[M + H]^+$ at *m/z* 332 and the proposed fragmentation scheme of S9P1.

Figure 12 Proposed in vitro metabolic pathways for pioglitazone. Bold indicates that metabolites M1, M2, M3, M7, M8, M11, and S9P1 were novel metabolites of pioglitazone.

DMD Fast Forward. Published on February 25, 2010 as DOI: 10.1124/dmd.109.031583
This article has not been copyedited and formatted. The final version may differ from this version.

Table 1 Positive ion LC/MS/MS data of metabolites of pioglitazone in freshly isolated human, rat, and monkey hepatocytes.

Metabolites	Retention time (min)	$[M + H]^+$ *m/z*	Product ions *m/z*	Freshly isolated hepatocytes		
				Human	Rat	Monkey
M1	7.8	361	119, 134, 254 (B)[a] , 280, 297	+[b]	+	+
M2	12.2	551	134, 286, 332 (B), 358, 375, 417	+	+	+
M3	13.2	377	119, 134, 254 (B), 280, 297	+	+	+
M4	14.5	373	132, 150 (B), 240, 256	+	ND[c]	+
M5	15.0	373	132, 135, 150 (B), 238, 355	+	+	+
M6	15.2	387	146, 164 (B)	+	+	+
M7	16.8	533	134, 357 (B)	+	+	+
M8	17.8	345	119, 134 (B), 240, 254, 280, 328	+	ND	+
M9	18.2	373	119, 134, 150, 240, 268 (B), 284, 313, 355	+	+	+
M10	19.4	373	133, 150, 210 (B), 222, 238, 239, 284, 355	+	+	+
M11	23.3	346	119, 134 (B), 254, 270, 286,	+	+	+
M12	23.9	355	132 (B), 210, 238, 239, 284	+	ND	+
M13	30.1	371	106, 148 (B), 254	+	+	+

[a]B: base peak.

[b]+: metabolite detected.

[c]ND: not detected.

Fig. 1

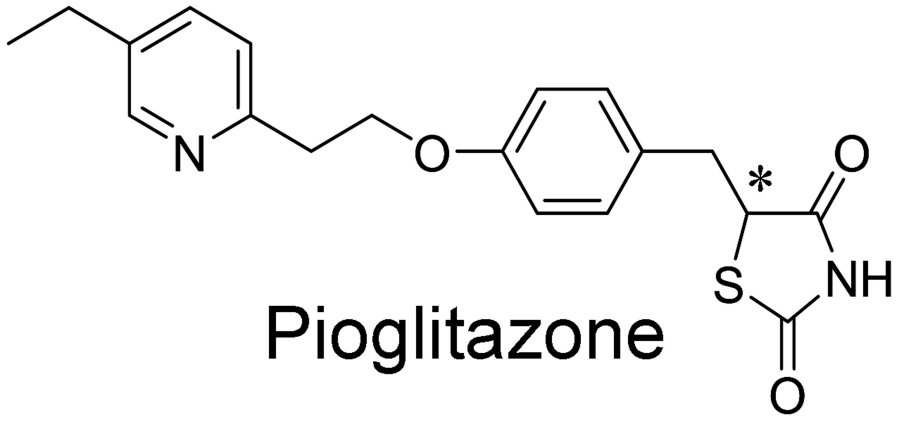

Pioglitazone

* indicates position of ^{14}C label

Fig. 2

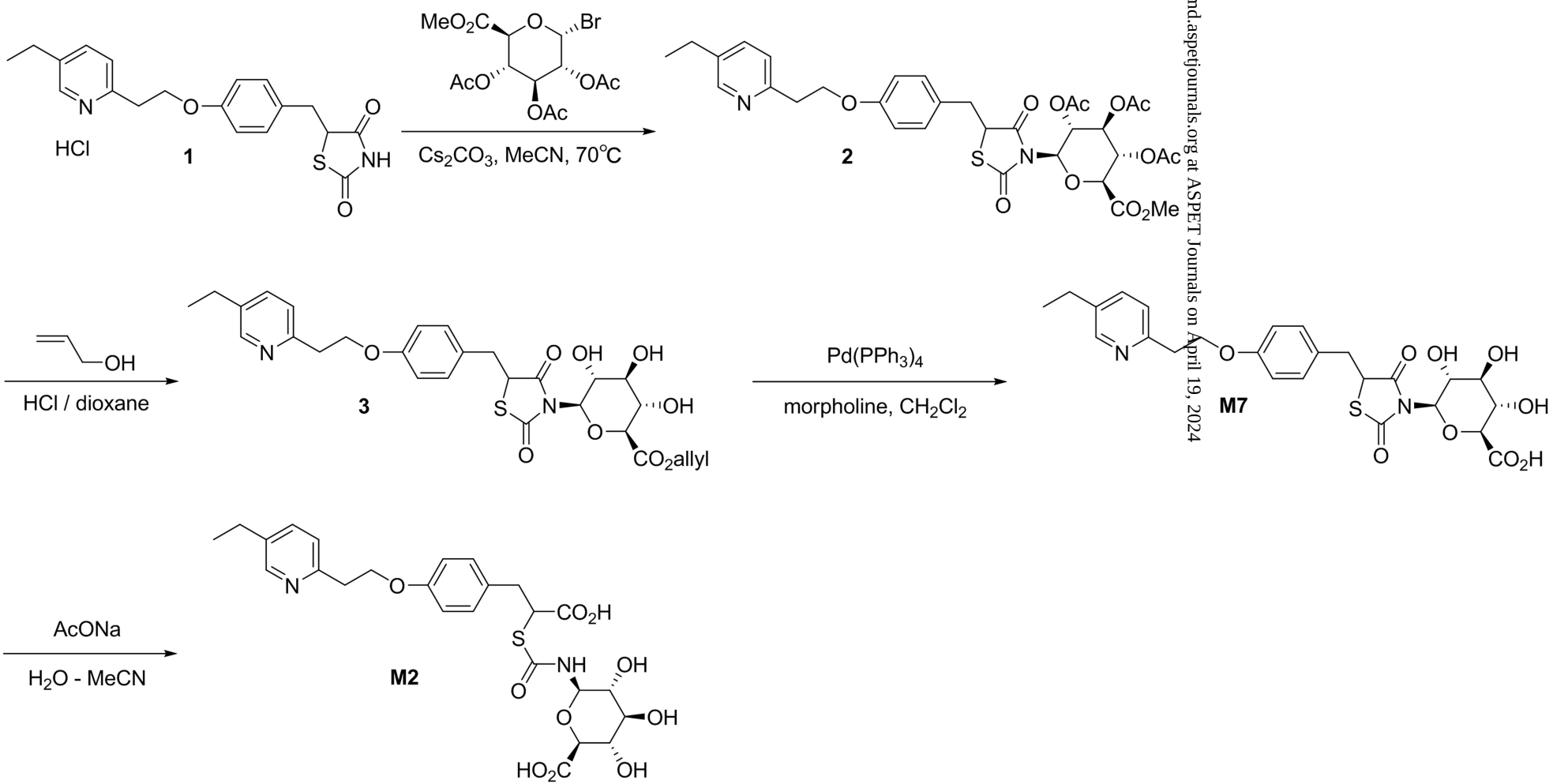

Fig. 3

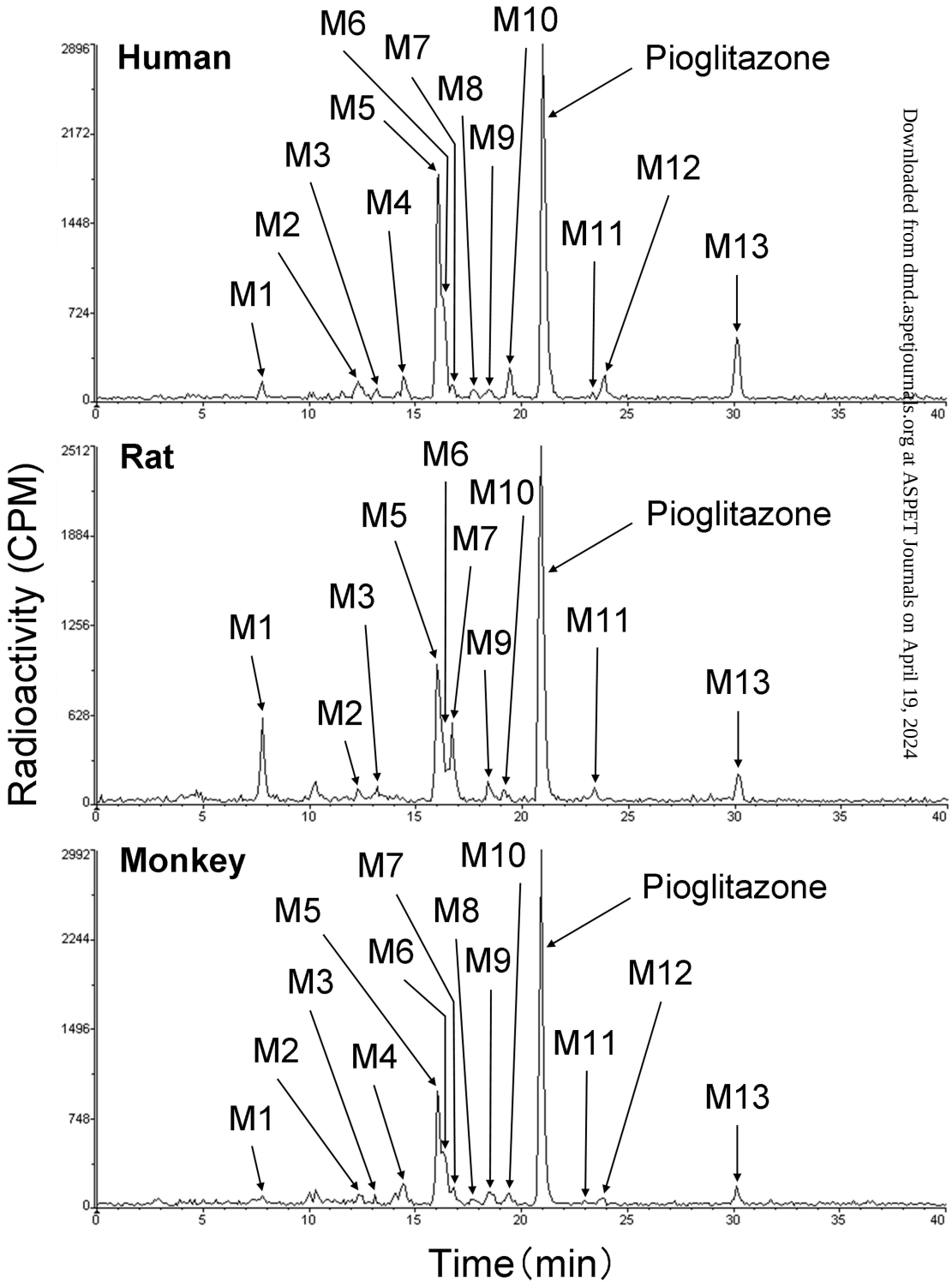

Fig. 4

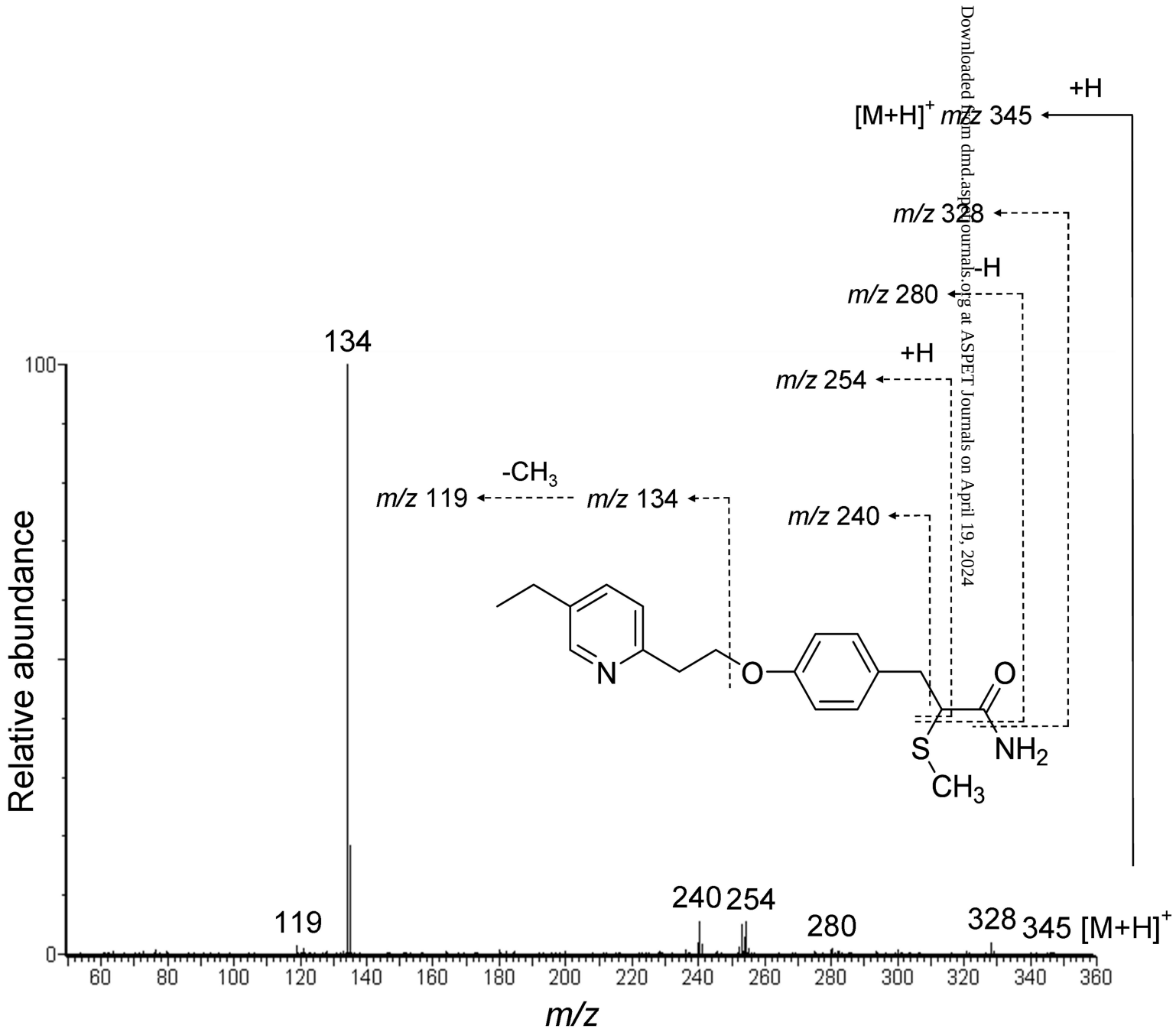

Fig. 5

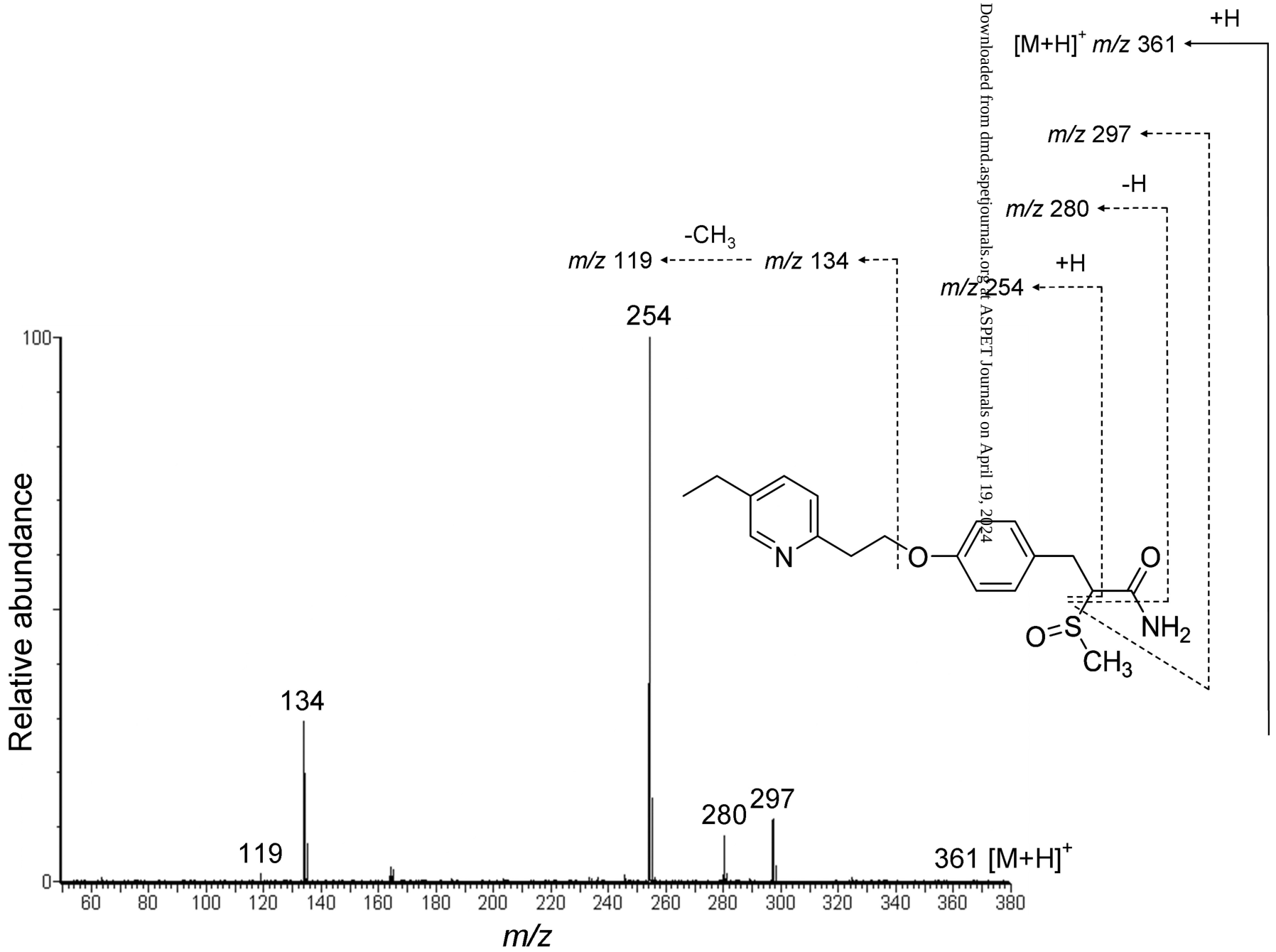

Fig. 6

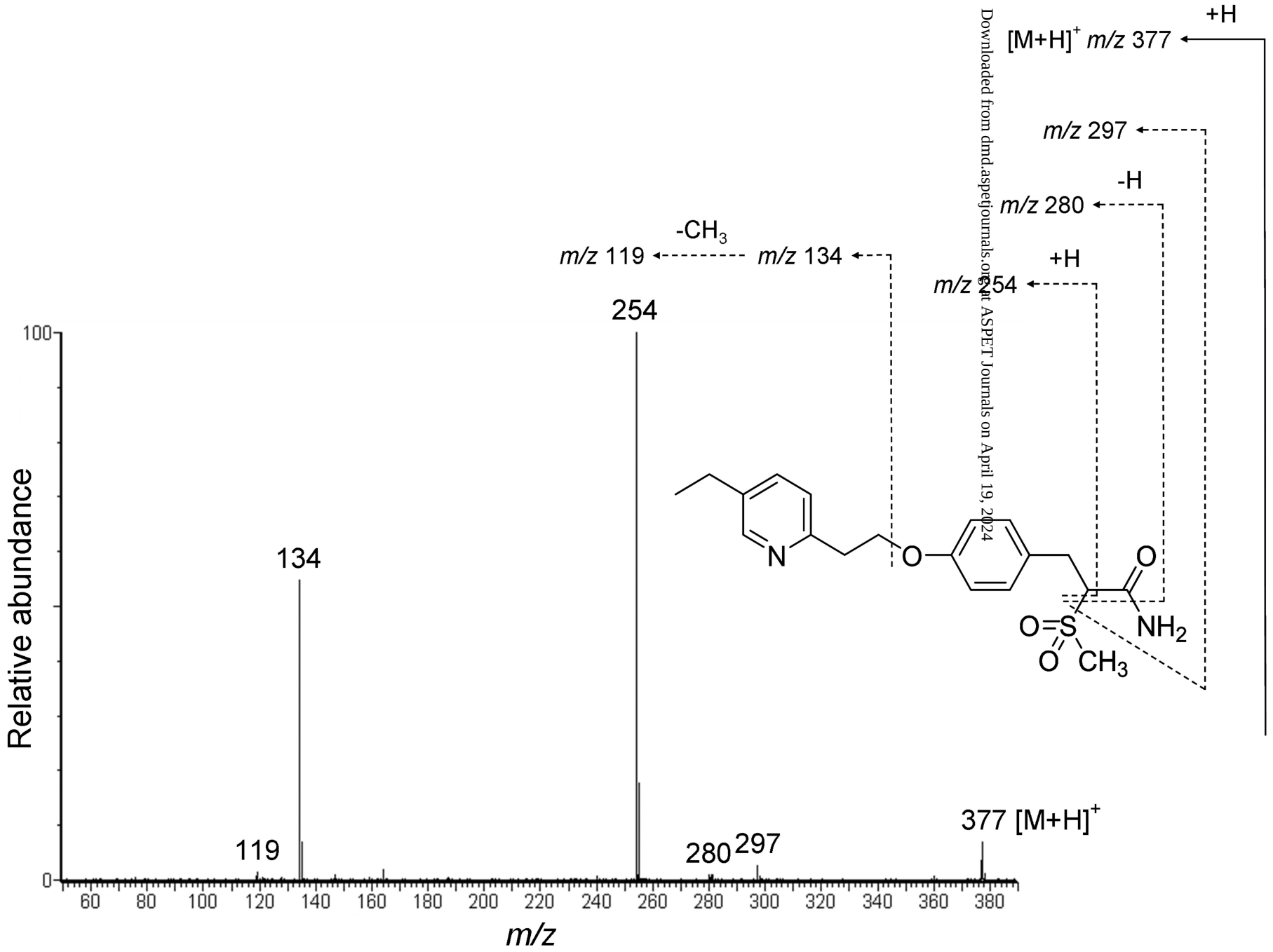

Fig. 7

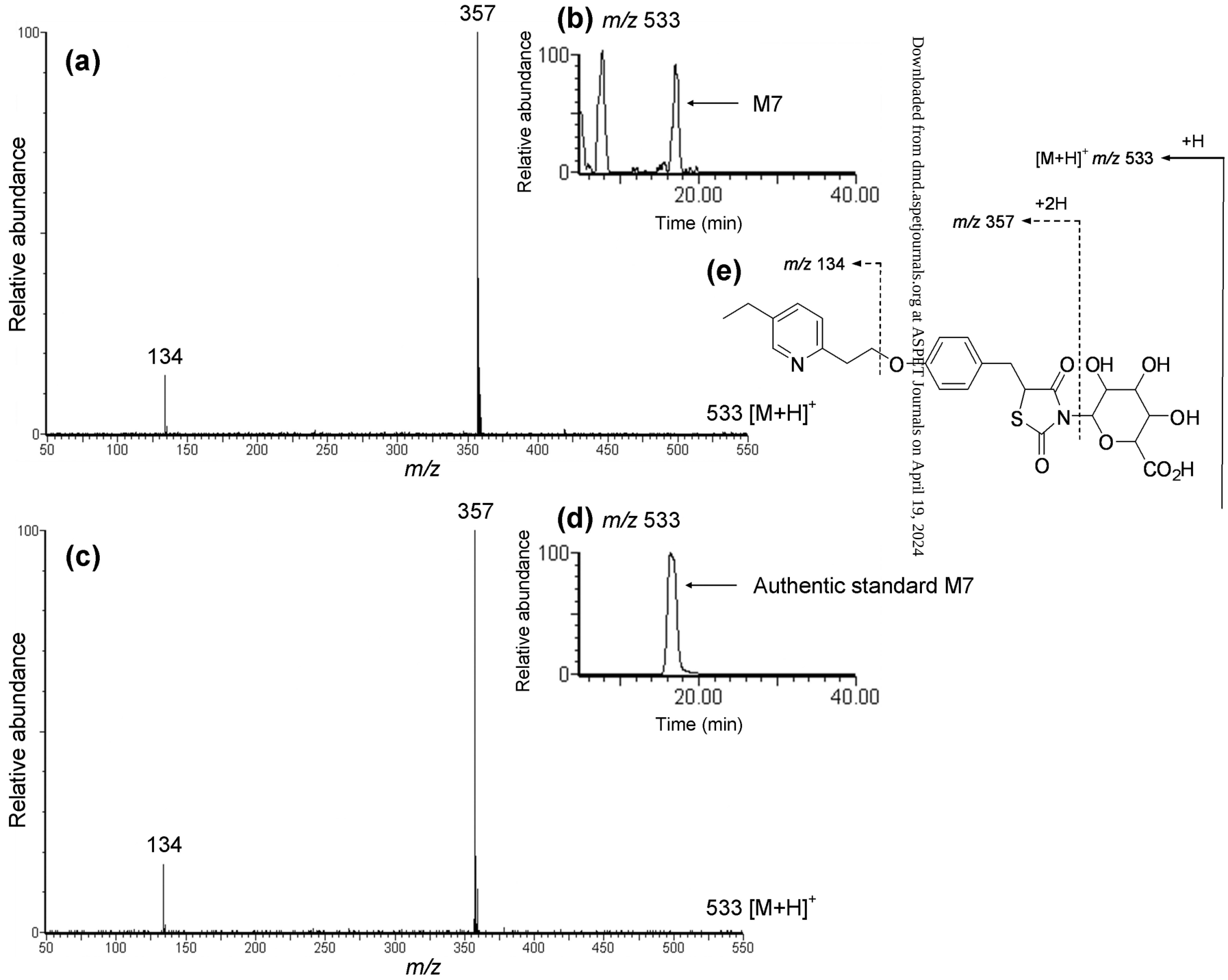

Fig. 8

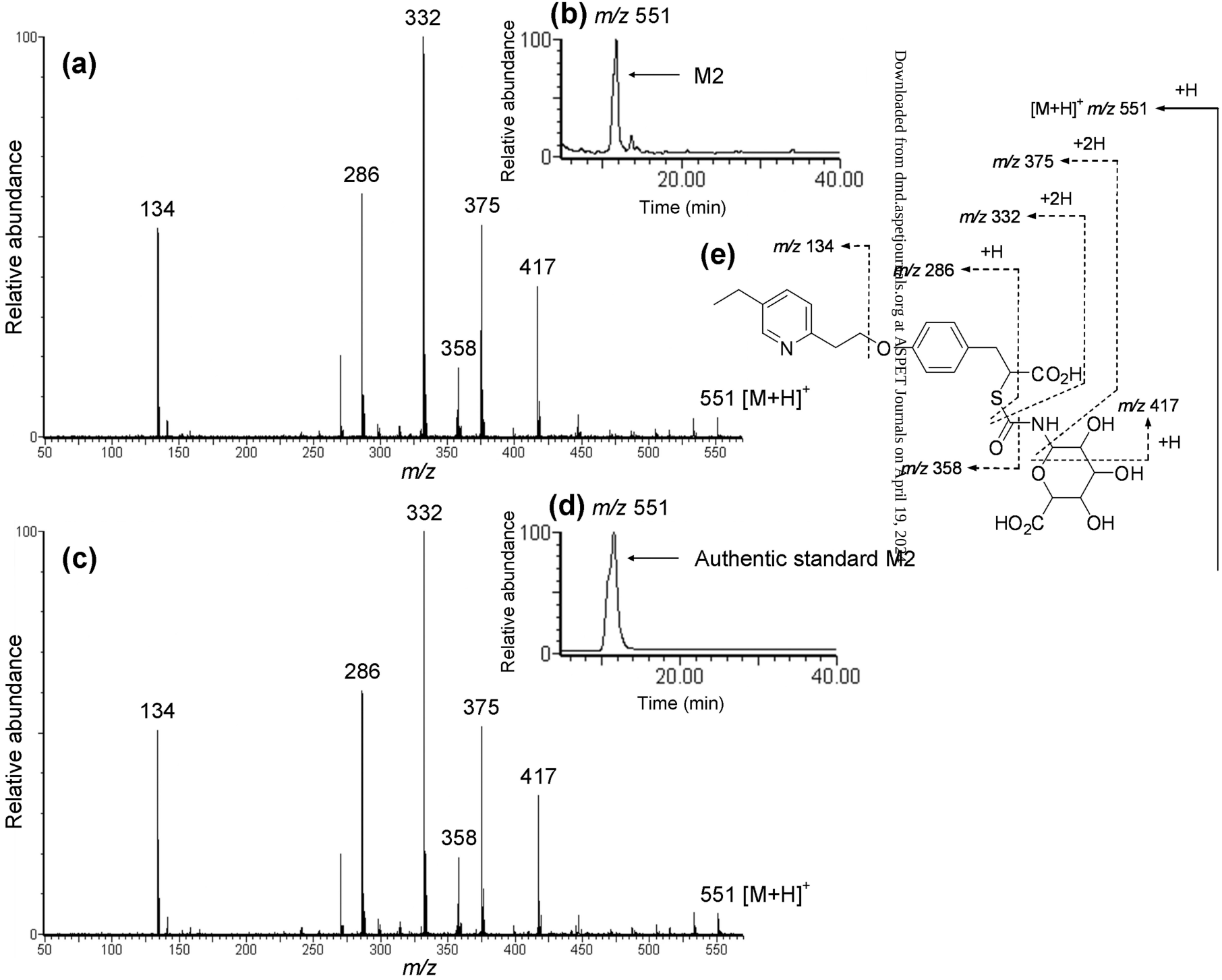

Fig. 9

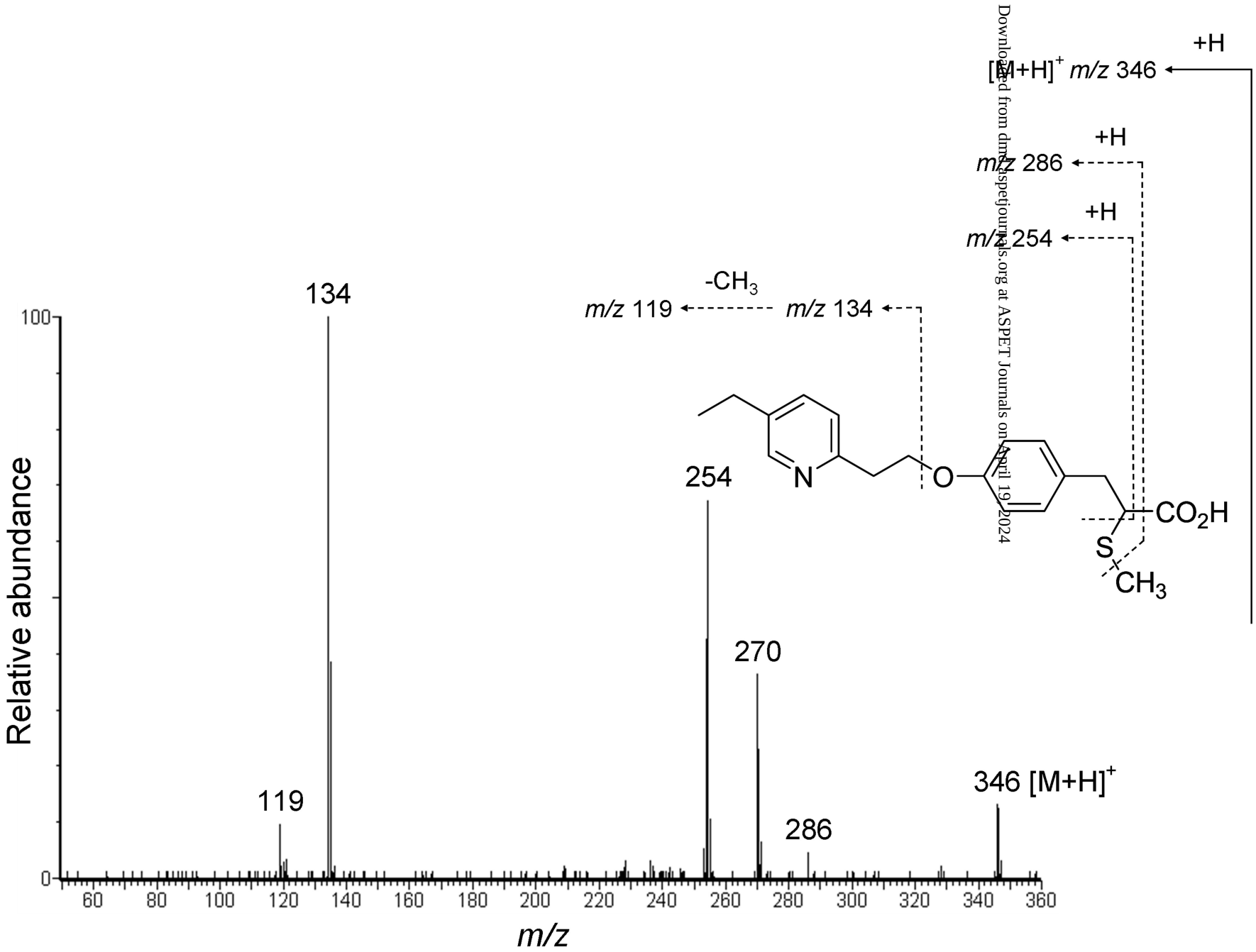

Fig. 10

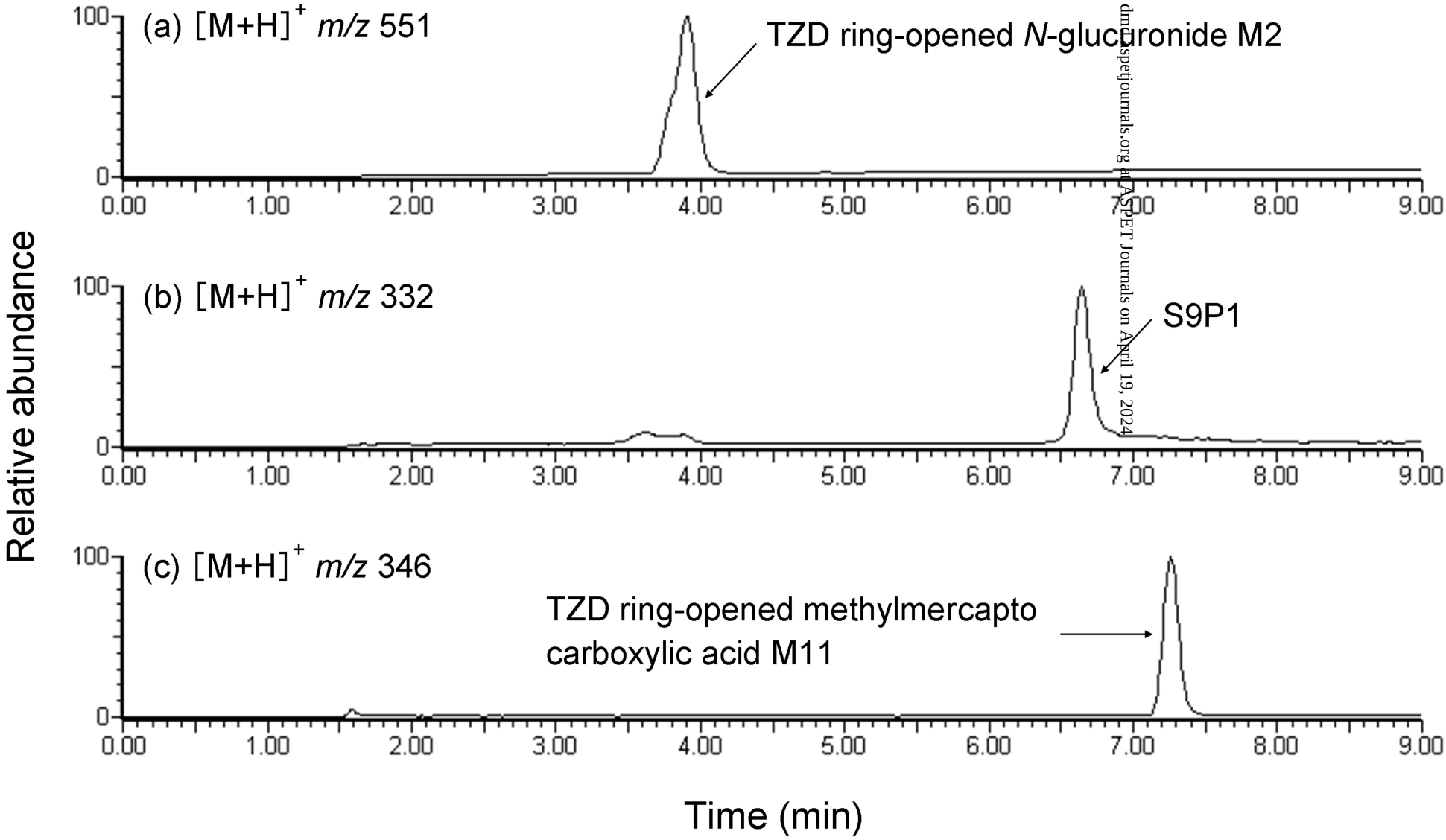

Fig. 11

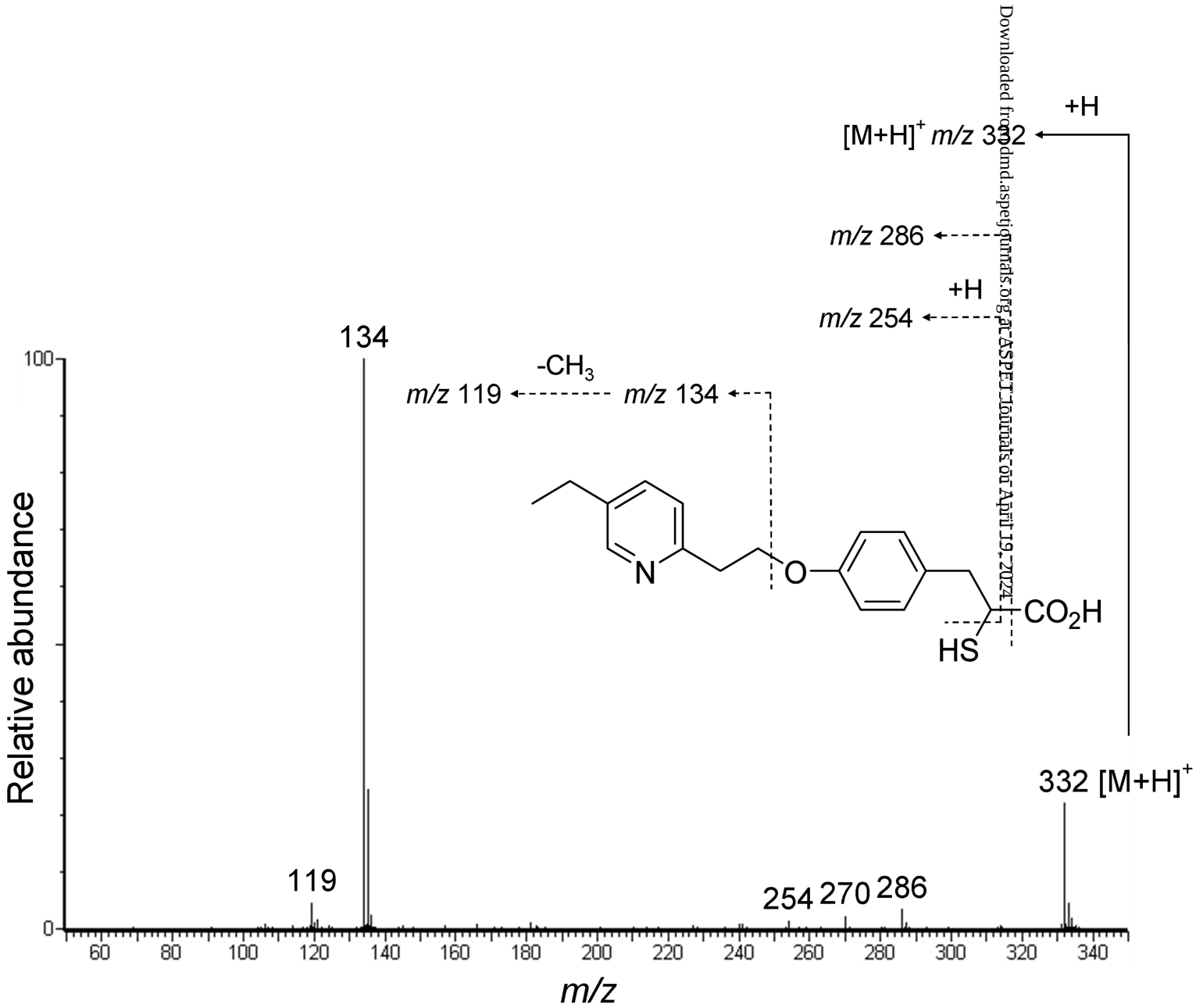

Fig. 12